https://doi.org/10.30799/jnst.244.19050410 J. Nanosci. Tech. - Volume 5 Issue 4 (2019) 780–783

ISSN: 2455-0191

Share Your Innovations through JACS Directory

Journal of Nanoscience and Technology

Visit Journal at http://www.jacsdirectory.com/jnst

Impedance and Electric Modulus Studies on Polyaniline/Nickel Ferrite (PANI/$NiFe_2O_4$) Composites

Ajai Kumar S. Molakeri[1,*], S. Sindhu[1], M. Shivalingayya[1], Sangappa K. Ganiger[2]

[1]*Department of Physics, Guru Nanak Dev Engineering College, Bidar – 585 403, Karnataka, India.*
[2]*Department of Physics, Government Engineering College, Raichur – 584 134, Karnataka, India.*

ARTICLEDETAILS

Article history:
Received 29 April 2019
Accepted 21 May 2019
Available online 12 June 2019

Keywords:
Impedance Spectroscopy
Electric Modulus
Nickel Ferrite

ABSTRACT

Conducting polyaniline/nickel ferrite (PANI/$NiFe_2O_4$) composites are synthesized by employing interfacial polymerization method. The composite has been synthesized with 10, 30 and 50 wt.% of nickel ferrites in PANI. The prepared samples were characterized by FTIR and SEM with EDS. The dominant peaks in FTIR graph confirm the formation of PANI/$NiFe_2O_4$ composites. The XRD pattern, confirms the formation of composites. The surface morphology of these composites was studied with scanning electron microscope (SEM). Impedance and electric modulus of these composites was investigated in the frequency range of 10^2 Hz to 10^6 Hz. It is found that Debye type relaxation has been confirmed by the Cole-Cole plot and electrical modulus is inversely proportional to the conductivity of these composites.

1. Introduction

The conducting polymers are a new group of synthetic polymers which combines the chemical and mechanical properties of polymers with the electronic properties of metals and semiconductors [1]. Conducting polymers are used in many applications such as microwave absorption, electronic displays, corrosion protection coating, electrochemical batteries, supercapacitors, sensors, and electrodes [2-6]. They have extended p -conjugation with single- and double-bond alteration along its chain. They behave as a semiconductor material with low charge carrier mobility [7] and their conductivity is increased to reach the metallic range by doping with appropriate dopants [7]. Polyaniline is the most widely studied conducting polymer because of its facile synthesis, low synthetic cost, high electrical conductivity, good environmental and thermal stability [8-12]. Polyaniline can be easily prepared either chemically or electrochemically from acidic aqueous solutions [13, 14]. The most common preparation method is by oxidative polymerization with ammonium peroxodisulfate as an oxidant.

Ferrites belong to a special class of magnetic materials, which have a wide range of technological applications. Due to their low cost, ferrite materials are used in various devices like microwave, transformer cores, magnetic memories, isolators, noise filters, etc [15-18]. The spin-glass state in ferrites exhibits the most interesting magnetic property that causes high field irreversibility, shift of the hysteresis loops, and anomalous relaxation dynamics [19, 20].

Nickel ferrite ($NiFe_2O_4$) is one of the most important spinel ferrites that have been studied. Stoichiometric $NiFe_2O_4$ considers as n-type semiconductor [21]. It exhibits different kinds of magnetic properties such as paramagnetic, superparamagnetic or ferrimagnetic behavior depending on the particle size and shape.

In our earlier paper, we reported AC conductivity and dielectric properties of PANI/$NiFe_2O_4$ composites [22] and in the present paper, the preparation of PANI/$NiFe_2O_4$ composites, its characterization through FTIR spectra, scanning electron microscope, impedance spectroscopy and electric modulus is reported.

2. Experimental Methods

2.1 Synthesis of Polyaniline/$NiFe_2O_4$ Composites

The polyaniline/$NiFe_2O_4$ composites were prepared via interfacial polymerization method with different weight percentage of $NiFe_2O_4$ (10, 30 and 50 wt.%). One gram of aniline was dissolved in 40 mL of $CHCl_3$. 0.1 M ammonium persulphate was dissolved in 1 M HCl and the $NiFe_2O_4$ particles prepared by combustion method in the weight percent of 10, 30 and 50 are added to the above mixture of aqueous and organic phase. After 5 minutes dark green precipitate formed slowly at the interface and then gradually diffused into aqueous phase. After 24 hours, the entire aqueous phase was filled homogeneously with dark green color film, organic layer observed shows orange color due to the formation of aniline oligomers. The aqueous phase was then collected and washed with ethanol and water to remove the unreacted aniline. The residue of polymer thus obtained is purified and dried in vacuum oven at 40 °C for 36 hours. In this way 3 different polyaniline – $NiFe_2O_4$ composites with different wt.% of $NiFe_2O_4$ in polyaniline have been synthesized as reported [22, 23]. The dried polymer composite sample was used for structural characterization and further used to study the electrical properties.

2.2 Characterization

The above synthesized samples were structurally and morphologically characterized by using different techniques like FTIR, XRD and SEM. The FTIR spectra of samples were recorded on ThermoNicolet, Avatar 370 spectrometer in KBr medium at room temperature. The X-ray diffraction patterns of the prepared samples were obtained by employing Bruker AXS D8 advance X-ray diffractometer using CuKα radiation (λ=1.5418 Å) in the 2θ range 10° to 65°. The surface morphology of polyaniline-$NiFe_2O_4$ composites were studied by using Joel model JSM-6390 LV scanning electron microscope (SEM). To measure the AC conductivity, the pellets of the prepared samples were coated with silver paste on either side was held between two nominally spring-loaded copper plates and the AC parameters were measured using N4L-PSM 1735 Numetri-Q programmable LCR meter in a frequency range 10 to 10^6 Hz.

3. Results and Discussion

3.1 FTIR Spectral Studies

Fig. 1(a) shows FTIR spectra of pure polyaniline and Fig. 1(b-d) shows that of polyaniline/nickel ferrite (10, 30 and 50 wt.%) respectively. Careful

*Corresponding Author:ajaymolakeri@gmail.com(Ajai Kumar S. Molakeri)

https://doi.org/10.30799/jnst.244.19050410

Cite this Article as: Ajai Kumar S. Molakeri, S. Sindhu, M. Shivalingayya, Sangappa K. Ganiger, Impedance and electric modulus studies on polyaniline/nickel ferrite (PANI/$NiFe_2O_4$) composites, J. Nanosci. Tech. 5(4) (2019) 780–783.

observation of Fig. 1(a) reveals the intensity peaks at 1564 cm^{-1} and 1478 cm^{-1} may be attributed due to the presence of C=C stretching of the quinonoid rings and C=C stretching of the benzenoid units of polymer respectively. The peak at 1301 cm^{-1} attributed to the secondary aromatic amine of C–N stretching. The peak 1244 cm^{-1} attributed to –N=quinoid=N- stretching. The peak 1137 cm^{-1} attributed to the measure of degree of electron delocalization. The peak 808 cm^{-1} attributed to the N–H out-of-plane bending [24].

Fig. 1(b-d) shows FTIR spectra of polyaniline/$NiFe_2O_4$ composite (10, 30 & 50 wt.% of $NiFe_2O_4$ in polyaniline), the prominent peaks that are observed at 816, 812, 808, 616, 618, 619 and 494, 459, 546 cm^{-1} indicating the well wrapping of $NiFe_2O_4$ particles with PANI in the composites [25]. It is also observed that the stretching frequencies are moved toward higher frequency side shows that $NiFe_2O_4$ particles are homogeneously distributed in the polymeric chain. This might be recognized because of the "van der Waals force" interaction amongst $NiFe_2O_4$ particles and polymeric chain. Table 1 shows Observed absorption bands of polyaniline and polyaniline/nickel ferrite composites.

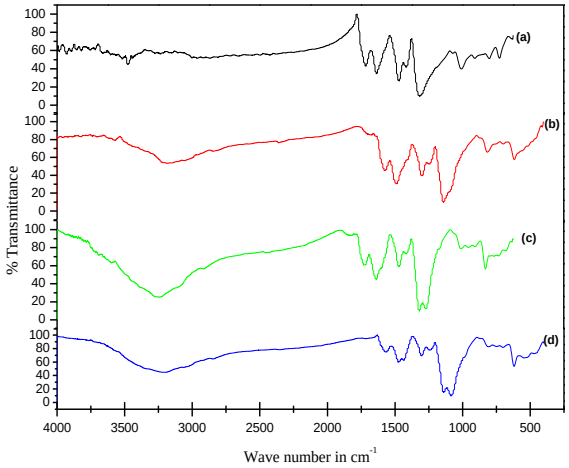

Fig. 1 FTIR spectra of (a) polyanilne (b-d) polyaniline/$NiFe_2O_4$ composites (10, 30 and 50 wt.% of $NiFe_2O_4$ in polyaniline)

Table 1 Absorption bands polyaniline and polyaniline – nickel ferrite composites

Sample	Vibrational assignments in cm^{-1}							
	Benzenic-quinonic nitrogen	C-C aromatic	Aromatic amine	-N= quinoid =N-	C-N-C	C-H out-of-plane	Tetra-hedral sites	Octa-hedral sites
PANI	1564	1478	1301	1244	1137	808	-	-
10 wt.%	1575	1491	1330	1299	1140	816	616	494
30 wt.%	1577	1479	1440	1301	1140	812	618	459
50 wt.%	1567	1472	1303	1241	1139	808	619	546

3.2 XRD Characterization

The X-ray diffraction pattern of polyaniline, pure $NiFe_2O_4$ and polyaniline – $NiFe_2O_4$ composite (50 wt.%) is shown in Fig.2. From Fig. 2(a) by investigating carefully, the X-ray diffraction proposes that polyaniline has amorphous nature with an expansive peak centered at 2θ = 20.7° and 25.29°. This is the distinctive peak of polyaniline, which is attributed to the periodicity in parallel and perpendicular directions of the polymer chains respectively [26]. XRD spectra of polyaniline, demonstrates an expansive reflection at lower Bragg angle 2θ estimation of 25.29° comparing to (200) diffraction plane of HCl doped PANI of ES-I structure [27, 28].

Fig. 2(b) shows the X-ray diffraction pattern of pure $NiFe_2O_4$ particles and Fig. 2(c) shows that of polyaniline – $NiFe_2O_4$ composite (50 wt.% of $NiFe_2O_4$ in polyaniline). It is seen from the figure that the intense peaks of $NiFe_2O_4$ indicate the crystalline nature of the particles (JCPDS No. 10-0325). The prominent peaks corresponding to 2θ = 29.98°, 35.38°, 36.97°, 43.00°, 49.18°, 53.79°, 57.23°, 62.63°, 63.76° and 75.12° are due to (220), (311), (222), (400), (331), (422), (511), (440), (531) and (533) crystal planes of $NiFe_2O_4$ respectively. By comparing the XRD patterns of the composite and $NiFe_2O_4$ particles, the peak intensity of the composites decreased when compared to pure $NiFe_2O_4$ which is due to the polymerization of polyaniline on the surface of $NiFe_2O_4$ [25]. The semi sharp peak of polyaniline at 25.29° has widened this is due to doping $NiFe_2O_4$ in polyaniline. This confirms the formation of composite material. The crystalline size was determined by Scherrer's formula [29]. The size of the $NiFe_2O_4$ particles were estimated over the range 25 to 33 nm and that of polyaniline–$NiFe_2O_4$ (50 wt.%) composite over the range 25-43 nm.

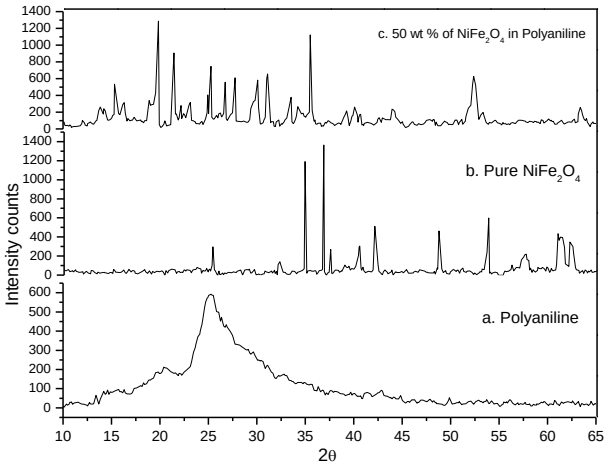

Fig. 2 X-Ray diffraction patterns of (a) polyaniline (b) pure $NiFe_2O_4$ (c) polyaniline – $NiFe_2O_4$ composite (50 wt.%)

3.3 SEM Study

Fig. 3 shows the SEM image of polyaniline/$NiFe_2O_4$ composite with 50 wt.% of $NiFe_2O_4$ in polyaniline. High magnification SEM image reveals that, the surface of composites was rough and exhibit, more or less, spherical morphology. From the image it is clear that, the PANI can minimize the aggregation of particles because of the repulsive force between magnetic particles and PANI. It also noticed that, the PANI layers are wrapped on the surface of $NiFe_2O_4$ particles appearing as small aggregated globules [30].

SEM images of samples were not well resolved, because samples are highly magnetic and intensity of electron beam of SEM may not be sufficient to provide the required resolution to make estimates of sample sizes. Particle size distribution was determined by using Image J software to obtain the maximum size distribution range by selected area of the SEM image of the samples.

Fig. 4 shows the particle size pie graph and the maximum size distribution range of polyaniline – $NiFe_2O_4$ composites are found to be 24 nm to 123 nm. An energy dispersive X-ray spectroscopy (EDS) analysis of polyaniline – $NiFe_2O_4$ composite (50 wt.%), it can be seen from the Fig. 5 and Table 2, the $NiFe_2O_4$ particles are uniformly dispersed in polyaniline. The presence of Ni, Fe and O elements in the EDS spectrum indicates the formation of composite along with small traces of sulphur and chlorine.

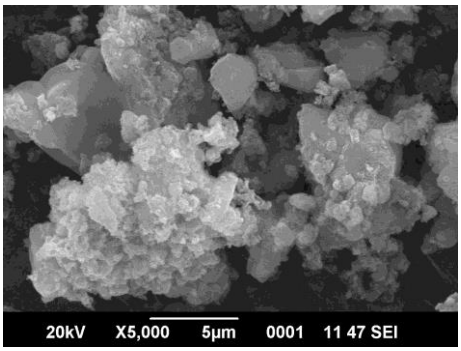

Fig. 3 SEM image of polyaniline – $NiFe_2O_4$ composite (50 wt %)

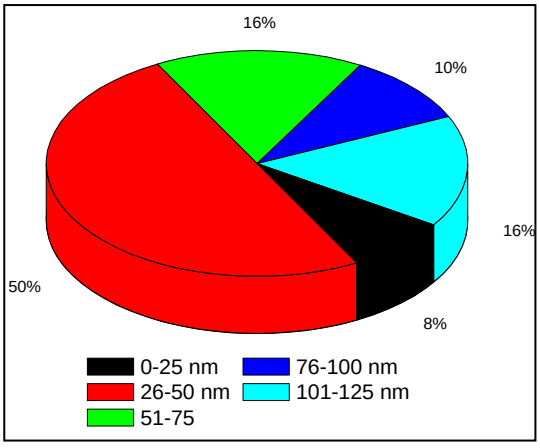

Fig. 4 Particle size pie graph and the maximum size distribution range of polyaniline – $NiFe_2O_4$ composites

https://doi.org/10.30799/jnst.244.19050410

Cite this Article as: Ajai Kumar S. Molakeri, S. Sindhu, M. Shivalingayya, Sangappa K. Ganiger, Impedance and electric modulus studies on polyaniline/nickel ferrite (PANI/$NiFe_2O_4$) composites, J. Nanosci. Tech. 5(4) (2019) 780–783.

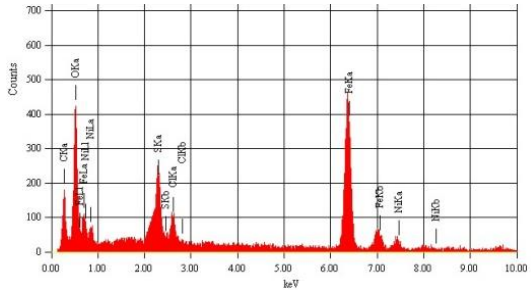

Fig. 5 EDS spectrum of polyaniline/$NiFe_2O_4$ composite (50 wt.%)

Table 2 EDS of PANI/$NiFe_2O_4$ (50 wt.%)

Element	Mass %	Atom %
C	15.35	35.31
O	15.51	26.78
S	7.56	6.52
Cl	3.58	2.79
Fe	54.47	26.95
Ni	3.53	1.66
Total	100	100

3.4 Impedance Spectral Studies

The real and imaginary part of impedance (Z' & Z") and electric modulus (M' & M") parameters have been calculated by the recorded values of equivalent capacitance (C_p), dissipation factor (D), phase angle (δ) and parallel equivalent resistance (R_p) using LCR meter at selected frequency range. Fig. 6 shows the variation of real impedance as a function of frequency of imaginary impedance (Cole-Cole plot) of polyaniline – $NiFe_2O_4$ composites. It is observed from the above graph that the semi circles of Cole-Cole plot suggest the dominance of Debye type relaxation has been confirmed. It is observed that resistance of the composites is inconsistent because of the change in the allotment of $NiFe_2O_4$ particles in polyaniline. A mechanism for the charge motion through the pressed pellets of conducting polymers was hypothesized. In the Fig. 7 the points on the diagram represent the experimental data, while the continuous line represents the polynomial fitting based on the non-linear least square fitting.

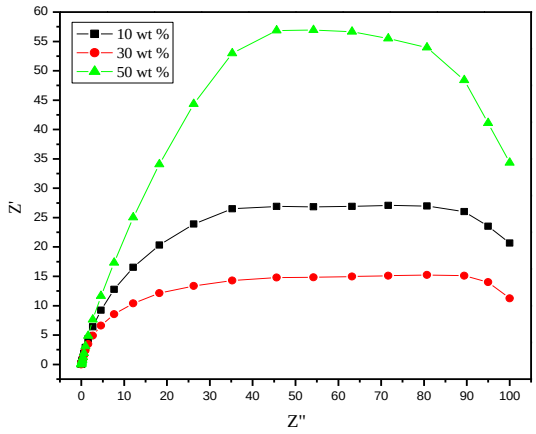

Fig. 6 Cole-Cole plot of polyaniline/$NiFe_2O_4$ composites (Z' as a function of Z")

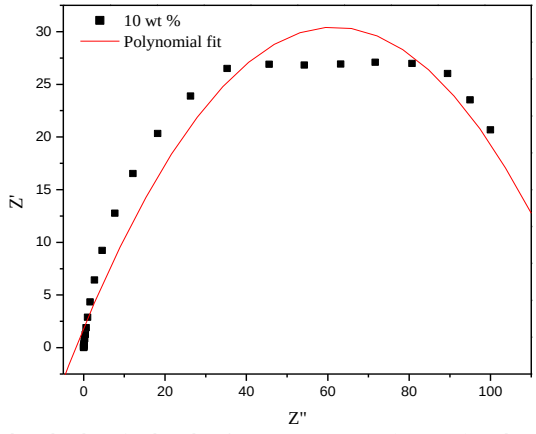

Fig. 7 Cole-Cole plot of polyaniline/$NiFe_2O_4$ composite (10 wt.%) with non-linear least square fitting

https://doi.org/10.30799/jnst.244.19050410

3.5 Electric Modulus

Fig. 8 shows the variation of real part of electric modulus as a function imaginary electric modulus (M' vs M") of Polyaniline /$NiFe_2O_4$ composites. It is observed that an arc with their centers at the origin and the radii of arcs seems to be varying with wt.% may be because of the changes in the allotment of $NiFe_2O_4$ particles in polyaniline. It has been reported that the radius of the arc of complete plane diagram is dependent on the electrical conductivity of the composites, as arc radius increases the conductivity decreases [31, 32].

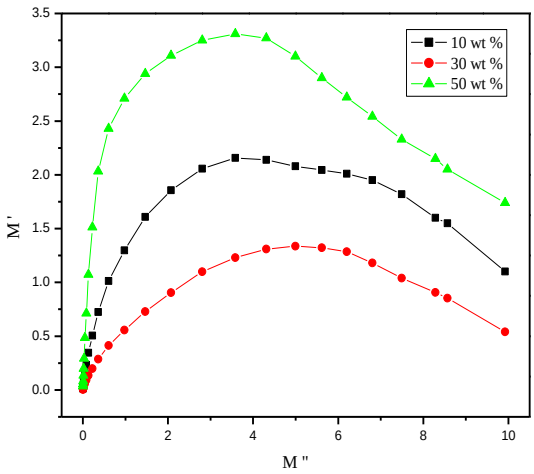

Fig. 8 Electric modulus plot of polyaniline/$NiFe_2O_4$ composites

4. Conclusion

Impedance and electric modulus studies on polyaniline/nickel ferrite (PANI/$NiFe_2O_4$) composites have been presented in this paper. The composites were synthesized by interfacial polymerization. The formation of composites is confirmed by FTIR it is observed that the stretching frequencies are moved toward higher frequency side shows that $NiFe_2O_4$ particles are homogeneously distributed in the polymeric chain. This might be recognized because of the "van der Waals force" interaction amongst $NiFe_2O_4$ particles and polymeric chain. From the XRD pattern, the semi sharp peak of polyaniline at 25.29° has widened this is due to doping $NiFe_2O_4$ in polyaniline which confirms the formation of composite material. The crystalline size of the $NiFe_2O_4$ particles were estimated over the range 25 to 33 nm and that of polyaniline – $NiFe_2O_4$ (50 wt.%) composite over the range 25 to 43 nm which are good agreement with SEM. The SEM images shows, the PANI can minimize the aggregation of particles because of the repulsive force between magnetic particles and PANI. It also shows that, the PANI layers are wrapped on the surface of $NiFe_2O_4$ particles appearing as small aggregated globules. The variation in real and imaginary impedance as a function of frequency of polyaniline/ $NiFe_2O_4$ composites Cole-Cole plot, it is observed that the semi circles suggest the dominance of Debye type relaxation has been confirmed. It is observed that resistance of the composites is inconsistent because of the change in the allotment of $NiFe_2O_4$ particles in polyaniline. The variation of real part of electric modulus as a function imaginary electric modulus (M' vs M") of polyaniline/$NiFe_2O_4$ composites, it is also observed that an arc with their centers at the origin and the radii of arcs seems to be varying with wt.% may be because of the changes in the allotment of $NiFe_2O_4$ particles in polyaniline.

References

[1] J. Anand, S. Palaniappan, D.N. Sathyanarayana, Conducting polyaniline blends and composites, Prog. Polym. Sci. 23 (1998) 993-1018.
[2] T.M. Akel, S. Pienimaa, T. Taka, S. Jussila, H. Isotalo, Thin polyaniline films in EMI shielding, Synth. Metals 85 (1997) 1335-1336.
[3] X. Lu, N.H. Ng, J. Xu, H. Chaobin, Electrical conductivity of polyaniline-dodecylobenzene sulphonic acid complex: Thermal degradation and its mechanism, Synth. Metals 128 (2002) 167-178.
[4] J.Q. Kan, X.H. Pan, C. Chen, Polyaniline-uricase biosensor prepared with template process, Biosens. Bioelectron. 19 (2004) 1635-1640.
[5] N. Ahmad, A.G. MacDiarmid, Inhibition of corrosion of steels with the exploitation of conducting polymers, Synth. Metals 78 (1996) 103-110.
[6] T.L. Rose, S.D. Antonio, M.H. Jillson, A.B. Kron, R. Suresh, F. Wang, A microwave shutter using conductive polymers, Synth. Metals 85 (1997) 1439-1440.
[7] K. Gupta, P.C. Jana, A.K. Meikap, Electrical transport and optical properties of the composite of polyaniline nanorod with gold, Solid State Sci. 14 (2012) 324-329.

[8] T. Machappa, M.V.N. Ambika Prasad, AC conductivity and dielectric behavior of polyaniline/sodium metavenadate (PANI/$NaVO_3$) composites, Phys. B. Condens. Matter. 404 (2009) 4168- 4172.
[9] H.S. Kim, H.L. Hobbs, L. Wang, M.J. Rutten, C.C. Wamser, Biocompatible composites of polyaniline nanofibers and collagen, Synth. Metals 159 (2009) 1313-1318.
[10] Y.F. Huang, C.W. Lin, Introduction of methanol in the formation of polyaniline nanotubes in an acid-free aqueous solution through a self-curling process, Polymer 50 (2009) 775-782.
[11] B.K. Sharma, A.K. Gupta, N. Khare, S.K. Dhawan, H.C. Gupta, Synthesis and characterization of polyaniline-ZnO composite and its dielectric behaviour, Synth. Metals 159 (2009) 391-395.
[12] E. Detsri, S.T. Dubas, Interfacial polymerization of water-soluble polyaniline and its assembly using the layer-by-layer technique, J. Met. Mater. Miner. 19 (2009) 39-44.
[13] N. Gospodinova, L. Terlemezyan, Conducting polymers prepared by oxidative polymerization: polyaniline, Prog. Polym. Sci. 23 (1998) 1443-1484.
[14] R.J. Mathew. D.L. Yang, B.R. Mattes, Effect of Elavated Temperature on the Reactivity and Structure of Polyaniline, Macromol. 35 (2002) 7575-7581.
[15] M. Hashim, Alimudin, S. Kumar, S.E. Shirsath, E.M. Mohamed, et al., Studies on the activation energy from the ac conductivity measurements of rubber ferrite composites containing manganese zinc ferrite, Physica B 407 (2012) 4097-4103.
[16] A. Goldman, Modern ferrite technology, 2nd Ed., Springer, New York, 2006.
[17] S.E. Shirsath, R.H. Kadam, S.M. Patange, M.L. Mane, A. Ghasemi, A. Morisako, Enhanced magnetic properties of Dy^{3+} substituted Ni-CuZn ferrite nanoparticles, Appl. Phys. Lett. 100 (2012) 042407-042410.
[18] A. Narayanaswamy. N. Sivakumar, Influence of mechanical milling and thermal annealing on electrical and magnetic properties of nanostructured Ni-Zn and cobalt ferrites, Bull. Mater. Sci. 31 (2008) 373-380.
[19] K. Raj, B. Moskoowitz, R. Casciari, Advances in ferrofluid technology, J. Magn. Magn. Mater. 149 (1995) 174-180.
[20] R.H. Kodama, C.L. Seaman, A.E. Berkowitz, M.B. Malpe, Low-temperature magnetic relaxation of organic coated $NiFe_2O_4$ particles, J. Appl. Phys. 75 (1994) 5639-5641.
[21] B. Baruwati, K. Reddy, S. Manorama, R. Singh, O. Prakash, Tailored conductivity behavior in nanocrystalline nickel ferrite, Appl. Phys. Lett. 85 (2004) 2833-2835.
[22] Ajai Kumar S. Molakeri, Sangshetty Kalyane, Preparation, structural and dielectric properties of polyaniline-nickel ferrite composites, Int. J. Mater. Sci. 12 (2017) 47-56.
[23] Ajai Kumar S. Molakeri, A.D. Shetkar, B. Raghunanda, Sangshetty Kalyane, Electrical and magnetic properties of polyaniline-nickel ferrite composites, Int. J. Emerg. Technol. 7 (2) (2016) 164-168.
[24] Jing Jiang, Facile synthesis and characterization of polyaniline/$NiFe_2O_4$ nanocomposite in w/o microemulsion, J. Macromol. Sci. B: Phys. 47 (2008) 242-249.
[25] B. Senthilkumar, K. Vijaya Sankar, C. Sanjeeviraja, R. Kalai Selvan, Synthesis and physico-chemical property evaluation of PANi-$NiFe_2O_4$ nanocomposite as electrodes for supercapacitors, J. Alloy Compd. 553 (2013) 350-357.
[26] J.P. Pouget, M.E. Jozefowicz, A.J. Epistein, X. Tang, A.G. MacDiarmid, X-ray structure of polyaniline, Macromol. 24 (1991) 779-789.
[27] J. Joo, S.M. Long, J.P. Pouget, E.J. Oh, A.G. MacDiarmid, A.J. Epstein, Charge transport of the mesoscopic metallic state in partially crystalline polyanilines, Phys. Rev. B 57 (1998) 9567-9580.
[28] H.C. Pant, M.K. Patra, S.C. Negi, A. Bhatia, S.R. Vadera, N. Kumar, Studies on conductivity and dielectric properties of polyaniline–zinc sulphide composites, Bull. Mater. Sci. 29 (2006) 379-384.
[29] T.J. Prosa, M.J. Winokur, Jeff Moulton, Paul Smith, A.J. Heeger, X-ray diffraction studies of the three-dimensional structure within iodine-intercalated poly(3-octylthiophene), Phys. Rev. B 51 (1995) 159-168.
[30] A.H. Elsayed, M.S. Mohy Eldin, A.M. Elsyed, A.H. Abo Elazm, E.M. Younes, H.A. Motaweh, Synthesis and properties of polyaniline/ferrites nanocomposites, Int. J. Electrochem. Sci. 6 (2011) 206-221.
[31] E.S. Matveeva, R. DiazCalleja, V.P. Parkhutik, Impedance study of chemically synthesized emeraldine form of polyaniline, Electrochim. Acta 41 (1996) 1351-1357.
[32] T. Machappa, M. Sasikala, M.V.N. Ambika Prasad, Impedance and electric modulus of conducting polyaniline/$ZnWO_4$ composites, Int. J. Sci. Res. 1 (2012) 113-115.

https://doi.org/10.30799/jnst.244.19050410

Cite this Article as: Ajai Kumar S. Molakeri, S. Sindhu, M. Shivalingayya, Sangappa K. Ganiger, Impedance and electric modulus studies on polyaniline/nickel ferrite (PANI/$NiFe_2O_4$) composites, J. Nanosci. Tech. 5(4) (2019) 780–783.